

# New Control of PV Solar Farm as STATCOM (PV-STATCOM) for Increasing Grid Power Transmission Limits During Night and Day

Rajiv K. Varma, *Senior Member, IEEE*, Shah Arifur Rahman, *Member, IEEE*,  
and Tim Vanderheide. *Member, IEEE*

**Abstract**—This paper presents a novel concept of utilizing PV solar farm inverter as STATCOM, termed PV-STATCOM, for improving stable power transfer limits of the interconnected transmission system. The entire inverter rating of PV solar farm which remains dormant in the nighttime is utilized with voltage and damping controls to enhance stable power transmission limits. During daytime, the inverter capacity left after real power production is used to accomplish the above objective. Transient stability studies are conducted on a realistic single machine infinite bus power system having a midpoint located PV-STATCOM using EMTDC/ PSCAD simulation software. The PV-STATCOM improves the stable transmission limits substantially in the night and also in the day even while generating large amounts of real power. Power transfer increases are also demonstrated in the same power system for i) two solar farms operating as PV-STATCOMs and ii) a solar farm as PV-STATCOM and an inverter based wind farm with similar STATCOM controls. This novel utilization of PV solar farm asset can thus improve power transmission limits which would have otherwise required expensive additional equipment such as, series/shunt capacitors, or separate Flexible AC Transmission System (FACTS) Controllers.

**Index Terms**—Photovoltaic solar power systems, inverter, voltage control, reactive power control, damping control, FACTS, STATCOM, transmission capacity, wind power system.

## I. INTRODUCTION

FLEXIBLE AC Transmission System (FACTS) Controllers are being increasingly considered to increase the available power transfer limits/capacity (ATC) of existing transmission lines [1]-[4], globally. A new research has been reported on the nighttime usage of a PV solar farm (when it is normally dormant) where a PV solar farm is utilized as a STATCOM – a FACTS Controller, for performing voltage control, thereby improving system performance and increasing grid connectivity of neighboring wind farms [5], [6]. A new voltage control has also been proposed on a PV solar farm to

act as a STATCOM for improving the power transmission capacity [7]. Although, papers [8],[9] have proposed voltage control functionality with PV systems, none have utilized the PV system for power transfer limit improvement. A full converter based wind turbine generator has recently been provided with FACTS capabilities for improved response during faults and fault ride through capabilities [10].

This paper proposes a novel voltage control together with auxiliary damping control for a grid connected PV solar farm inverter to act as a STATCOM both during night and day for increasing transient stability and consequently the power transmission limit. This technology of utilizing a PV solar farm as a STATCOM is termed “PV-STATCOM”. It utilizes the entire solar farm inverter capacity in the night and the remainder inverter capacity after real power generation during the day, both of which remain unused in conventional solar farm operation. Similar STATCOM control functionality can also be implemented in inverter based wind turbine generators during no-wind or partial wind scenarios for improving the transient stability of the system. Studies are performed for two variants of a Single Machine Infinite Bus (SMIB) system. One SMIB system uses only a single PV solar farm as PV-STATCOM connected at the midpoint whereas the other system uses a combination of a PV-STATCOM and another PV-STATCOM or an inverter based wind Distributed Generator (DG) with similar STATCOM functionality. Three-phase fault studies are conducted using the electromagnetic transient software EMTDC/PSCAD, and the improvement in stable power transmission limit is investigated for different combinations of STATCOM controllers on the solar and wind farm inverters, both during night and day.

Section II describes the study systems. The results for various fault studies are presented in Section III. Performances of different proposed controls both during daytime and nighttime, are presented. The implications of implementing this new PV-STATCOM technology on large scale solar systems are described in Section IV, while the conclusions are presented in Section IV.

## II. SYSTEM MODELS

The single line diagrams of two study systems - Study System 1 and Study System 2 are depicted in Fig. 1 (a) and Fig. 1(b), respectively. Both systems are Single Machine Infinite Bus (SMIB) systems in which a large equivalent synchronous generator (1110 MVA) supplies power to the

---

The financial support from Ontario Centres of Excellence (OCE), Bluewater Power, Sarnia, and Hydro One under the grants WE-SP109-E50712-08 and CR-SG30-11182-11; and that from NSERC are gratefully acknowledged.

Rajiv K. Varma and S. A. Rahman are with the Department of Electrical and Computer Engineering, University of Western Ontario, London, Ontario, N6A 5B9, Canada (e-mail: rkvarma@uwo.ca; srahma32@uwo.ca). Tim Vanderheide is with Bluewater Power Renewable Energy Inc., Sarnia, Ontario, Canada (e-mail: TVanderheide@bluewaterpower.com).

infinite bus over a 200 km, 400 kV transmission line. This line length is typical of a long line carrying bulk power in Ontario. In Study System 1, a 100 MW PV solar farm (DG) as STATCOM (PV-STATCOM) is connected at the midpoint of the transmission line. In Study System 2, two 100 MVA inverter based Distributed Generators (DGs) are connected at 1/3<sup>rd</sup> (bus 5) and 2/3<sup>rd</sup> (bus 6) of line length from the synchronous generator. The DG connected at bus 6 is a PV-STATCOM and the other DG at bus 5 is either a PV-STATCOM or a wind farm with STATCOM functionality. In this case, the wind farm employs Permanent Magnet Synchronous Generator (PMSG) based wind turbine generators with full ac-dc-ac converter. It is understood that both the solar DG and wind DG employ several inverters. However, for this analysis, each DG is considered to have a single equivalent inverter with the rating equal to the total rating of solar DG or wind DG, respectively. The wind DG and solar DG are considered to be of the same rating, hence can be interchanged in terms of location depending upon the studies being performed. Fig. 2 presents the block diagrams of various subsystems of the two equivalent DGs. All the system parameters are given in [1].

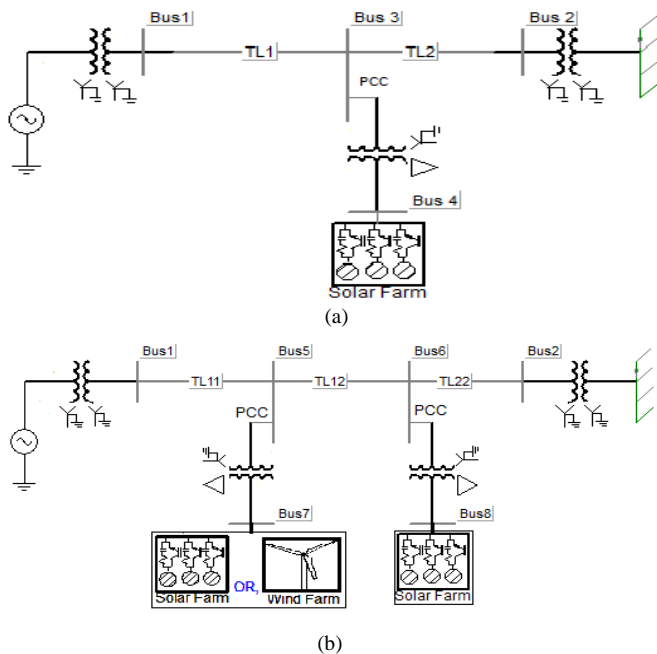


Fig. 1. Single line diagram of (a) Study system I with single solar farm (DG) and (b) Study System II with a solar farm (DG) and a solar/wind farm (DG).

### A. System Model

The synchronous generator is represented by a detailed sixth order model and a DC1A type exciter [1]. The transmission line segments TL1, TL2, TL11, TL12 and TL22 shown in Fig. 1 are represented by lumped pi-circuits. The PV solar DG, as shown in Fig. 2, is modeled as an equivalent voltage sourced inverter along with controlled current source as the DC source which follows the I-V characteristics of Photovoltaic (PV) panels [11]. The wind DG is likewise modeled as an equivalent voltage sourced inverter. In the solar DG, the DC power is provided by the solar panels, whereas in the full converter based wind DG, the DC power comes out of

a controlled AC-DC rectifier connected to the PMSG wind turbines, depicted as “wind Turbine-Generator-Rectifier (T-G-R)”. The DC power produced by each DG is fed into the DC bus of the corresponding inverter, as illustrated in Fig. 2. A maximum power point tracking (MPPT) algorithm based on incremental conductance algorithm [12] is used to operate the solar DGs at its maximum power point all the time and is integrated with the inverter controller [11]. The wind DG is also assumed to operate at its maximum power point, as this proposed control utilizes only the inverter capacity left after the maximum power point operation of both the solar DG and wind DG.

For PV-STATCOM operation during nighttime, the solar panels are disconnected from the inverter and a small amount of real power is drawn from the grid to charge the DC capacitor. The voltage source inverter in each DG is composed of six IGBTs and associated snubber circuits as shown in Fig. 2. An appropriately large DC capacitor of size 200 Farad is selected to reduce the DC side ripple [13]. Each phase has a pair of IGBT devices which converts the DC voltage into a series of variable width pulsating voltages, using the sinusoidal pulse width modulation (SPWM) technique [14]. An L-C-L filter [13] is also connected at the inverter AC side.

### B. Control System

#### B.1 Conventional Reactive Power Control:

The conventional reactive power control only regulates the reactive power output of the inverter such that it can perform unity power factor operation along with the DC link voltage control [15]. The switching signals for the inverter switching are generated through two current control loops in d-q-0 coordinate system [15, 16]. The inverter operates in conventional controller mode only provided that ‘Switch-2’ is in ‘OFF’ position. In this simulation, the voltage vector is aligned with the quadrature axis, i.e.,  $V_d=0$  [15, 16], hence,  $Q_{ref}$  is only proportional to  $I_d$  which sets the reference  $I_{d\_ref}$  for the upper control loop involving PI1. Meanwhile, the quadrature axis component  $I_q$  is used for DC link voltage control through two PI controllers (PI-2 and PI-3) [14,16] shown in Fig. 2(b) according to the set point voltage provided by the MPPT and as well as injects all the available real power ‘P’ to the network [15]. To generate the proper IGBT switching signals (gt1, gt2, gt3, gt4, gt5, gt6), the d-q components (md and mq) of the modulating signal are converted into three phase sinusoidal modulating signals and compared with a high frequency (5 kHz) fixed magnitude triangular wave or carrier signal.

#### B.2 PCC Voltage Control:

In the *PCC voltage control* mode of operation, the PCC voltage is controlled through reactive power exchange between the DG inverter and the grid. The conventional ‘Q’ control channel is replaced by the PCC voltage controller in Fig. 2 (b), simply by switching the ‘Switch-1’ to the position ‘A’. Hence, the measured signal,  $V_{PCC}$ , at the PCC is compared with the preset reference value  $V_{PCC\_ref}$  and is passed through the PI regulator, PI-4, to generate  $I_{d\_ref}$ .

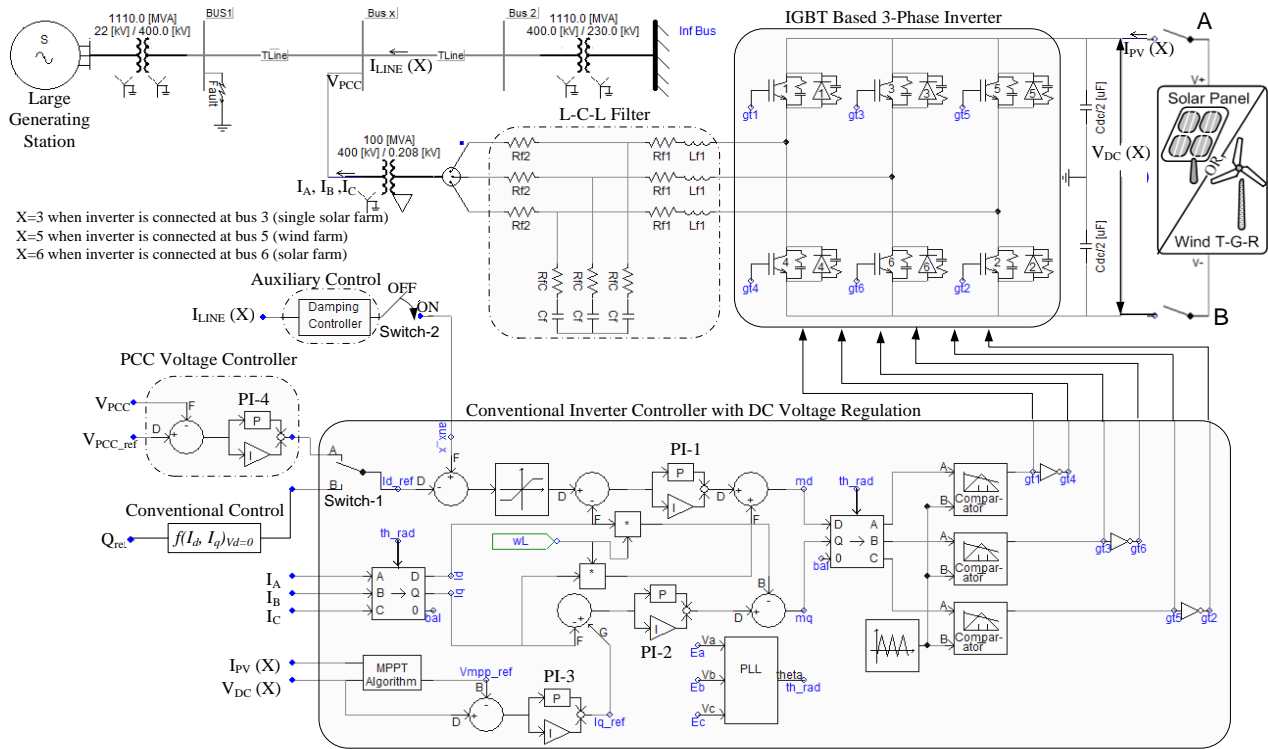


Fig. 2. Complete DG (solar/wind) system model with damping controller and PCC voltage control system.

The rest of the controller remains unchanged. The upper current control loop is used to regulate the PCC voltage whereas the lower current control loop is used for DC voltage control and as well as for supply of DG power to the grid. The amount of reactive power flow from the inverter to the grid depends on set point voltage at PCC. The parameters of the PCC voltage controller are tuned by systematic trial and error method to achieve the fastest step response, least settling time and a maximum overshoot of 10-15%. The parameters of all the controllers are given in Appendix.

### B.3 Damping Control:

A novel auxiliary *damping controller* is added to the PV control system and shown in in Fig. 2. (b). This controller utilizes line current magnitude as the control signal. The output of this controller is added with the signal  $I_{d\_ref}$ . The transfer function of this damping controller is expressed as in [19]:

$$F_D = G \cdot \frac{sT_w}{1 + sT_w} \cdot \left( \frac{1 + sT_1}{1 + sT_2} \right) \dots \dots \dots (3)$$

The transfer function comprises a gain, a washout stage, and a 1<sup>st</sup> order lead-lag compensator block. This controller is utilized to damp the rotor mode oscillations of the synchronous generator and thereby improve system transient stability. The damping controller is activated by toggling ‘Switch-2’ to the ‘ON’ position. This damping controller can operate in conjunction with either the conventional reactive power

control mode or with the PCC voltage control mode by toggling the ‘Switch-1’ to position ‘B’ or ‘A’, respectively.

At first the base case generator operating power level is selected for performing the damping control design studies. This power level is considered equal to the transient stability limit of the system with the solar farm being disconnected at night. At this operating power level, if a three phase fault occurs at Bus 1, the generator power oscillations decay with a damping ratio of 5%. The solar farm is now connected and operated in the PV-STATCOM mode. The parameters of the damping controller  $F_D$  are selected as follows. The washout time constant  $T_w$  is chosen to allow the generator electromechanical oscillations in the frequency range up to 2 Hz to pass through [19]. The gain  $G$ , time constants  $T_1$  and  $T_2$  are sequentially tuned to get the fastest settling time of the electromechanical oscillations at the base case generator power level through repetitive PSCAD/EMTDC simulations. Thus the best combination of the controller parameters is obtained with a systematic hit and trial technique, and the parameters are given in the Appendix. It is emphasized that these controller parameters are not optimal and better parameters could be obtained by following more rigorous control-design techniques [19-20]. However, the objective of this paper is only to demonstrate a new concept of using a PV solar farm inverter as a STATCOM using these reasonably good controller parameters. In this controller, although line current magnitude signal is used, other local or remote signals which reflect the generator rotor mode oscillations [1] may also be utilized.

### III. SYSTEM STUDIES

Transient stability studies are carried out using PSCAD/EMTDC simulation software, for both the study systems during night and day, by applying a 3-Line to Ground (3LG) fault at bus 1 for 5 cycles. The damping ratio is used to express the rate of decay of the amplitude of oscillation [20]. For an oscillatory mode having an eigenvalue of  $\sigma + j\omega$ , the damping ratio  $\xi$  is defined as,

$$\xi = -\frac{\sigma}{\sqrt{\sigma^2 + \omega^2}}, \text{ and } \sigma = \frac{1}{\tau} \dots\dots\dots (4)$$

where,  $\tau$  is the time constant.

Therefore, for a 5% damping ratio of the rotor mode having oscillation frequency of 0.95 Hz, as considered in this study, the post-fault clearance settling time of the oscillations to come within 5% (typically within 3 times the time constant) of its steady state value [1], [20] is almost 10 seconds. The peak overshoot of PCC voltage is should also be limited within 1.1 pu of nominal voltage. The maximum stable generator power limit for the system is determined through transient stability studies for different modes of operation of the solar DG in study system 1, and those of the solar DG and the solar/winds DGs in study system 2.

#### A. Case Study 1: Power Transfer Limits in Study System 1

##### A.1 Conventional Reactive Power Control with the Novel Damping Control

In this study, the solar DG is assumed to operate with its conventional reactive power controller the DG operates at near unity power factor. For the nighttime operation of solar DG, the DC sources (solar arrays) are disconnected and the solar DG inverter is connected to the grid using appropriate controllers, as described below. Power transmission limits are now determined for the following four cases. The stable power transmission limits obtained from transient stability studies and the corresponding load flow results are presented in Table I where  $-ve Q$  represents the inductive power drawn and  $+ve Q$  represents capacitive power injected into the network.

##### i) solar DG operation during night with conventional reactive power controller:

The maximum stable power output from the generator  $P_g$  is 731 MW when the solar DG is simply sitting idle during night and is disconnected from the network. This power flow level is chosen to be the base value against which the improvements in power flow with different proposed controllers are compared and illustrated later in Table III. The real power from generator  $P_g$  and that entering into the infinite bus  $P_{inf}$  for this fault study are shown in Fig. 3(a). The sending end voltage at generator is shown in Fig 3(b) which shows voltage overshoot of 1.1pu.

##### ii) solar DG operation during night with damping controller:

The quantities  $P_g$ ,  $P_{inf}$ ,  $P_{solar}$ , and  $Q_{solar}$  are illustrated in Fig. 4(a). The damping controller utilizes the full rating of the DG inverter at night to provide controlled reactive power  $Q_{solar}$  and effectively damps the generator rotor mode oscillations. The voltages at generator bus  $V_g$  and at PCC bus  $V_{rms(PCC)}$  are depicted in Fig. 4(b). A very small amount of negative power flow from the solar farm  $P_{solar}$  is observed during night time.

This reflects the losses in the inverter IGBT switches, transformer and filter resistances caused by the flow of real current from the grid into the solar farm inverter to charge the DC link capacitor and maintain its voltage constant while operating the PV inverter as STATCOM with the damping controller (or even with voltage controller). During nighttime, the reference DC Link voltage  $V_{mpp\_ref}$  is chosen around the typical daytime rated maximum power point (MPP) voltage .

The oscillations in the solar PV power output during nighttime, as seen in Fig. 4, are due to the active power exchanged by the solar inverter both during the charge and discharge cycles in trying to maintain a constant voltage across the DC link capacitor, thereby enabling the inverter to operate as a STATCOM.

##### iii) solar DG operation during day with conventional reactive power controller:

The conventional control of a PV solar DG does not seem to alter the stable transmission limit in any appreciable manner.

##### iv) solar DG operation during day with damping controller:

The quantities  $P_g$ ,  $P_{inf}$ ,  $P_{solar}$ , and  $Q_{solar}$  are shown for the cases without damping controller and with damping controller in Figs. 5 and 6, respectively. The available inverter capacity after real power generation of 91 MW is,  $Q = \sqrt{(S^2 - P^2)} = 41.5$  MVar, which is used for damping oscillations during daytime.

The power transfer capacity increase in the daytime is expected to be lower than the nighttime, as only a part of the total inverter capacity is available for damping control during the day. However, it is noticed from Table I that the maximum power transfer during night time (850 MW) is actually less than the maximum power transfer value during day time (861 MW) This is because of an additional constraint that while increasing the power transfer, the overshoot in PCC voltage should not exceed 1.1 pu. If the power transfer is allowed until its damping ratio limit of 5% regardless of voltage overshoot, the maximum nighttime power transfer is observed to be 964MW whereas the maximum daytime power transfer is expectedly seen to be lower at 940MW (plots not shown).

**TABLE I**  
**Power Flows and Voltages for Study System I for Solar DG with conventional Reactive Power Control and Proposed Damping Control both during Nighttime and Daytime ( $V_g=1.05$  pu)**

Simulation Description		Gen. Bus	PCC/Middle Bus (3)			Inf. Bus
			$P_g$ (MW)	$V_{pcc}$ (pu)	$P_{solar}$ (MW)	
Nighttime	Conventional Operation of Solar DG	<b>731</b>	1.010	0	0	<b>-708</b>
	Solar DG with damping controller	<b>850</b>	1.000	-0.20	0.08	<b>-819</b>
Daytime	Conventional Operation of Solar DG	<b>730</b>	1.010	<b>19.0</b>	-0.50	<b>-725</b>
	Operation of Solar DG	<b>719</b>	1.008	<b>91.0</b>	-0.20	<b>-786</b>
	Solar DG with damping controller	<b>851</b>	1.000	<b>19.0</b>	-0.06	<b>-839</b>
		<b>861</b>	0.994	<b>91.0</b>	-0.20	<b>-917</b>

##### A.2 PCC Voltage Control with the Novel Damping Control

Transient stability results for a new control strategy involving PCC voltage control together with damping control. are shown in Table II for the following four cases:

*i) solar DG operation during night with voltage controller*

The increase in power transfer limit is dependent upon the choice of reference values for PCC voltage  $V_{pcc}$ . In the best scenario when  $V_{pcc}$  is regulated to 1.01 pu, the maximum power output from the generator increases to 833 MW, as compared to 731 MW when the solar DG operates with conventional reactive power control.

*ii) solar DG operation during day with voltage controller*

The power transfer increases for both low (19 MW) and high (91 MW) power output from the solar farm are seen to be highly sensitive to the PCC bus voltage setpoint. It is also noted that with lower availability of reactive power capacity after real power production, the ability to change the bus voltage is limited, which leads to a lower increase in power transmission capacity.

*iii) solar DG operation during night with both voltage and damping controller*

The generator and infinite bus power are depicted in Fig. 7(a), and corresponding voltages are shown in Fig. 7 (b). Although, rotor mode oscillations settle faster, the power transfer cannot be improved beyond 899 MW due to high overshoot in voltages.

*iv) solar DG operation during day with both voltage and damping controller.*

A further increase in power transfer is observed when both voltage control and damping control are employed, as compared to case (ii) when only voltage controller is utilized.

**TABLE II**

**Power Flows and Voltages for Study System I for Solar DG with Proposed PCC Voltage Control and Damping Control both during Nighttime and Daytime ( $V_g=1.05$  pu)**

Simulation Description	Gen. Bus	PCC/Middle Bus (3)			Inf. Bus	
	$P_g$ (MW)	$V_{pcc}$ (pu)	$P_{solar}$ (MW)	$Q_{solar}$ (MVar)	$P_{inf}$ (MW)	
Nighttime Solar DG with voltage controller	<b>789</b>	0.988	-1.5	-95.8	<b>-761</b>	
	<b>824</b>	0.990	-0.8	-66.0	<b>-793</b>	
	<b>830</b>	1.000	-0.3	-9.5	<b>-801</b>	
	<b>833</b>	1.010	-0.5	46.8	<b>-803</b>	
	<b>803</b>	1.022	-1.5	99.0	<b>-775</b>	
	<b>855</b>	1.000	-0.3	4.0	<b>-824</b>	
Nighttime Solar DG with both voltage and damping controller	<b>899</b>	1.010	-1.2	85.0	<b>-866</b>	
	<b>781</b>	0.990	<b>19.0</b>	-90.0	<b>-773</b>	
Daytime Solar DG with voltage controller	<b>815</b>	1.000	<b>19.0</b>	-13.7	<b>-804</b>	
	<b>782</b>	1.021	<b>19.0</b>	86.0	<b>-775</b>	
	<b>726</b>	0.99	<b>91.0</b>	-43.0	<b>-792</b>	
	<b>719</b>	1.000	<b>91.0</b>	-44.0	<b>-786</b>	
	Daytime Solar DG with both voltage and damping controller	<b>823</b>	1.000	<b>19.0</b>	-9.0	<b>-813</b>
		<b>755</b>	1.000	<b>91.0</b>	-41.0	<b>-817</b>

**TABLE III**

**Increase in Stable Power Transfer Limit (MW) for Study System I with Different PV-STATCOM Controls**

PV STATCOM CONTROL	NIGHT	DAY	
		Solar Power Output 19 MW	Solar Power Output 91 MW
Voltage Control	102	85	7
Damping Control	119	<b>121</b>	<b>142</b>
Voltage Control with Damping Control	<b>168</b>	93	36

For Study System 1, the net increase in power transfer capability as achieved with different PV-STATCOM controls in comparison with that obtained conventional reactive power control of the solar DG, is summarized in Table III.

The maximum increase in power transfer limit during nighttime is achieved with a combination of voltage control and damping control, whereas the same during daytime is accomplished with damping control alone. This is because in the night the entire MVA rating of the solar DG inverter is available for reactive power exchange, which can be utilized for achieving the appropriate voltage profile at PCC conducive for increasing the power transfer, as well as for increasing the damping of oscillations.

During daytime, firstly, the generation of real power from the solar DG tends to increase the voltage at PCC [5] and secondly, the net reactive power availability also gets reduced especially with large solar real power outputs. Therefore, it becomes difficult with limited reactive power to accomplish the appropriate voltage profile at PCC for maximum power transfer and also to impart adequate damping to the oscillations. However, if only damping control is exercised during daytime, power transfer limits appear to improve with higher real power outputs from the solar DG. This is because real power generation increases the PCC voltage which can be potentially helpful in increasing the power transfer capacity.

Since damping control is found more effective during daytime, the same is explored further for the following studies.

*B. Case Study 2: Power Transfer Limits in Study System II*

In this study, the proposed damping control strategy is compared with the conventional reactive power control strategy for Study System II shown in Fig. 1(b). A three phase to ground fault of 5 cycles is applied to generator bus at  $t = 8$  sec. The power transfer limits obtained through transient stability studies for different cases are illustrated in Table IV. The following eight cases are studied:

*B.1 Nighttime:*

i) Case 1 - None of the DGs generate real power  
The maximum power transfer limit is 731 MW as in Table I.

ii) Case 2 - Only wind DG generates real power. Both DGs operate with conventional reactive power control  
The power transfer limit decreases slightly with increasing wind power output.

iii) Case 3 - None of the DGs generate real power but both DGs operate with damping control

The different variables, generator power  $P_g$ , infinite bus power  $P_{inf}$ , real power of wind DG  $P_{wind}$ , reactive power of the wind DG  $Q_{wind}$ , real power of the solar DG  $P_{solar}$ , and the reactive power of the solar DG  $Q_{solar}$  are illustrated in Figure 8. Even though the entire ratings (100 MVar) of the wind DG and solar DG inverters are not completely utilized for damping control, the power transfer limit increases significantly to 960 MW.

iv) Case 4 - Only wind DG generates real power but both DGs operate on damping control  
There is only a marginal improvement in power limit with decreasing power output from the wind DG.

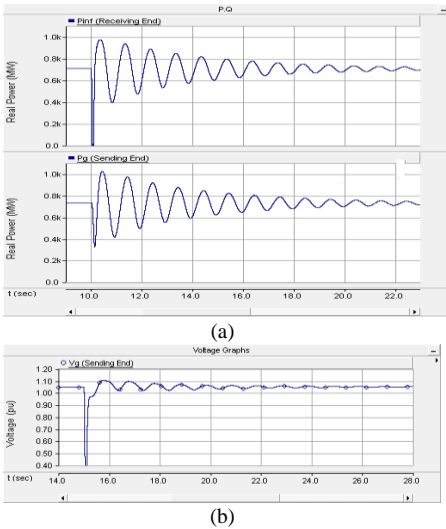


Fig. 3. (a) Maximum nighttime power transfer (731 MW) from generator when solar DG remains idle (b) Voltage at generator terminal.

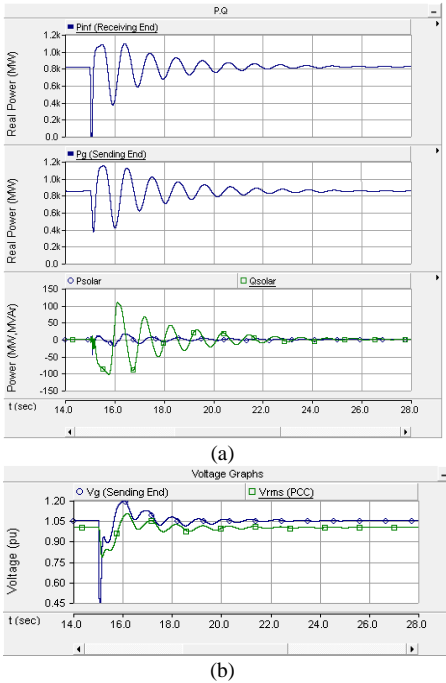


Fig. 4(a) Maximum nighttime power transfer (850 MW) from generator with solar DG using damping controller, (b) Voltages at generator terminal and DG PCC.

### B.2 Daytime:

- i) Case 5 - Both DGs generate real power  
The power transfer limit from the generator decreases as the power output from both DGs increase.
- ii) Case 6 - Only solar DG generates power  
The power transfer limit from the generator decreases as the power output from the solar DG increases. However, no substantial changes in power limits are observed as compared to the case when both DGs generate power (Case 5).

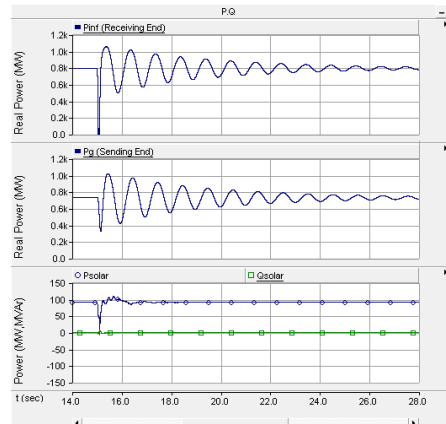


Fig. 5. Maximum daytime power transfer (719 MW) from generator with solar DG generating 91 MW real power.

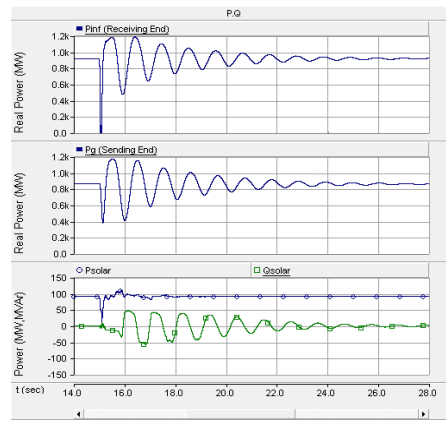
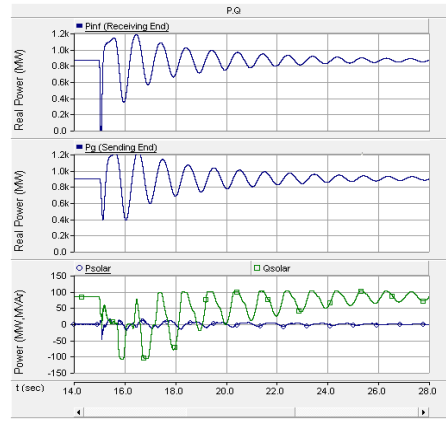


Fig. 6. Maximum daytime power transfer (861 MW) from generator with solar DG generating 91 MW real power and using the damping controller.



(a)

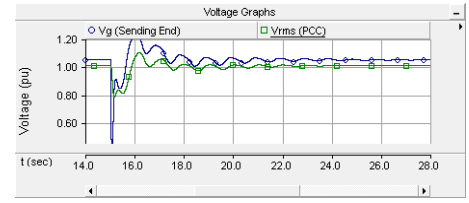


Fig. 7. (a) Maximum nighttime power transfer (899 MW) from generator while the solar DG uses damping controller with voltage control and (b) Voltages at generator terminal and solar DG PCC (1.01 pu).

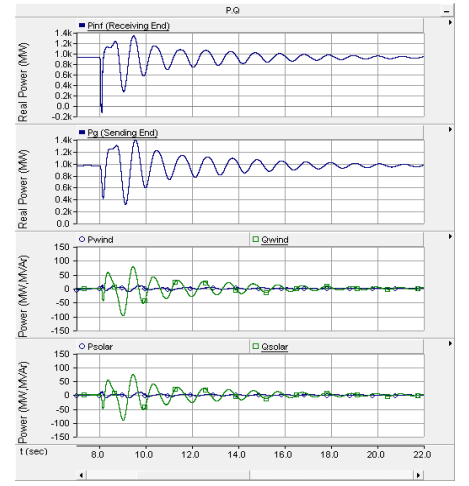


Fig. 8. Maximum nighttime power transfer from generator with both DGs using damping controller but with no real power generation.

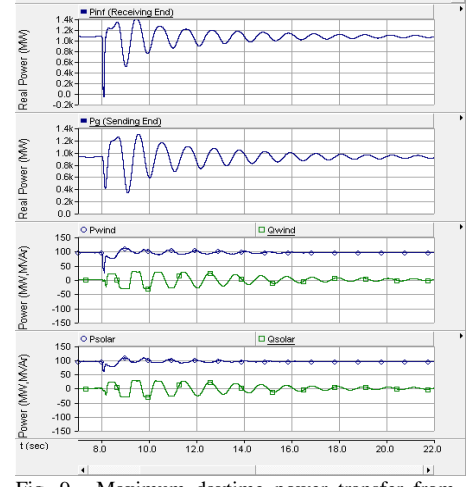


Fig. 9. Maximum daytime power transfer from generator while both DGs generate 95MW each using damping controller.

- iii) Case 7 - Both DGs generate real power and operate on damping control.

This case is illustrated by different variables  $P_g$ ,  $P_{inf}$ ,  $P_{wind}$ ,  $Q_{wind}$ ,  $P_{solar}$ , and  $Q_{solar}$  in Figure 9. The power limit does not change much with increasing power output from both DGs.

- iv) Case 8 - Only solar DG generates real power but both the DGs operate on damping control.

The power limit does not appear to change much with increasing power output from the solar DG.

**TABLE IV**

**Power Flows and Voltages for Study System II for both Solar DG and Wind DG with Conventional Reactive Power Control and Proposed Damping Control both during Nighttime and Daytime (Vg =1.05 pu)**

Control system	Gen. Bus	Wind DG at Bus (5)		Solar DG at Bus (6)		Inf. Bus	
	Pg (MW)	Vwnd (pu)	Pwnd (MW)	Vsol (pu)	Psol (MW)	Pinf (MW)	
Nighttime (P <sub>solar</sub> = 0)	Conventional Control	Case 1- None of the DGs generate real power					
		731	1.019	0	1.004	0	-708
		Case 2- Only wind DG generates real power but both DGs operate with conventional reactive power control					
		716	1.017	95	1.01	0	-785
	with damping controller.	729	1.018	20	1.003	0	-726
		Case 3- None of the DGs generate real power but both DGs operate with damping control					
		960	0.998	-0.7	0.982	-0.2	-918
		Case 4- Only wind DG generates real power but both DGs operate on damping control					
Daytime (P <sub>solar</sub> ≠ 0)	Conventional Control	Case 5- Both DGs generate real power					
		700	1.016	95	1.000	95	-865
		726	1.019	20	1.004	20	-743
		Case 6- Only solar DG generates power					
	with damping controller.	719	1.017	0	1.002	95	-790
		730	1.018	0	1.003	20	-727
		Case 7- Both DGs generate real power with damping control.					
		930	0.99	95	0.972	95	-1073
with damping controller.	923	1.0	20	0.983	20	-924	
	Case 8 - Only solar DG generates real power but both DGs operate on damping control.						
	938	0.998	-0.5	0.98	95	-991	
	944	0.999	-0.3	0.982	20	-925	

For Study System 2, the net increases in power transfer limits accomplished with the proposed novel damping control for different real power outputs from both DGs as compared to those attained with the conventional operation of both DGs, are depicted in Table V. The proposed damping control on the two DGs (of rating 100 MW each) in the nighttime increases the power transfer limits substantially by about 220 MW. This is expected as in the night the entire inverter MVA rating of both the DGs is available for damping control. The improvement is slightly less when wind DG produces high power. This is also expected as the reactive power availability decreases with the wind DG power output. During daytime, the proposed damping control on both the DGs also increases the power transfer limits substantially. A greater increase is seen during high power generation by any DG, as high power output improves the PCC voltage profile which assists in increasing the power transfer capacity.

**TABLE V**

**Increase in Power Transfer Limits for Study System II with Different DG Power Outputs**

DG Real Power Outputs (MW)	Power Limit Increase (MW)
<b>NIGHT</b>	
P <sub>solar</sub> = 0; P <sub>wind</sub> = 0	229
P <sub>solar</sub> = 0; P <sub>wind</sub> = 20	219
P <sub>solar</sub> = 0; P <sub>wind</sub> = 95	220
<b>DAY</b>	
P <sub>solar</sub> = 20; P <sub>wind</sub> = 20	197
P <sub>solar</sub> = 95; P <sub>wind</sub> = 95	230
P <sub>solar</sub> = 20; P <sub>wind</sub> = 0	214
P <sub>solar</sub> = 95; P <sub>wind</sub> = 0	219

#### IV. IMPLEMENTATION OF PV-STATCOM ON LARGE SCALE SOLAR SYSTEMS

The PV-STATCOM technology will be showcased, for the first time in a utility network of Ontario on a 10 kW PV solar system. The 10 kW solar system will be utilized for voltage regulation and power factor correction in addition to generating real power. Several detailed testing and validation studies are required to be completed before the PV-STATCOM will be allowed to connect to the wires of the utility. These include (i) PV-STATCOM controller testing with PSCAD/EMTDC simulation studies, (ii) Controller validation using Real Time Digital Simulation (RTDS) [21], and finally, full scale 10 kW Lab scale demonstration of the PV-STATCOM. Other Lab tests would be performed to meet requirements of IEEE standard 1547 [22].

The path for implementing PV-STATCOM technology in large real scale solar power systems is much more complex than that for the 10 kW systems. Major issues have to be examined and addressed. With respect to inverter technologies, adapting the PV-STATCOM concept to different configurations of inverters – 6 pulse, multipulse, multilevel, etc., and control coordination amongst multiple inverters in a PV solar plant, with each operating in PV-STATCOM mode, need to be addressed. Grid connection issues, such as, Protection and Control, Voltage Rise and Harmonics, Short Circuit Current Limitations, Disconnection during faults or staying connected with Low Voltage Ride Through (LVRT) Capabilities, need to be examined. Retrofitting PV inverters in large solar plants with PV-STATCOM technology will have to deal with warranty issues of inverters, in addition to revalidation of the solar system performance with the new PV-STATCOM retrofit. Another aspect is conformance to standards, such as, IEEE 1547 and its planned updates.

#### V. PRACTICALITY OF UTILIZING LARGE SCALE SOLAR FARMS FOR ENHANCING TRANSMISSION LIMITS

The number of large solar farms is increasing worldwide. There are at least four operating solar farms of rating 100 MW, three of which are connected at transmission level voltages [23] with more to follow [24,25]. The 550 MW Desert Sunlight Solar Farm Project in California will connect to the California's existing 500 kV transmission grid [26]. The Grand Renewable Energy Park in Ontario, Canada, has a 100 MW solar farm connected to the 230kV transmission line [27]. Meanwhile, several new transmission lines are being constructed worldwide to enhance power transfer capacity in transmission corridors [28]. Examples of new lines for carrying power from renewable sources are SWIP project [29], CREZ initiative [4], BPA system [30]. Evidently, these new lines are being constructed due to inadequate power transfer capacity in these corridors. There is therefore a potential opportunity for the large scale solar farms connected to such lines to provide the much needed increase in power transmission capacity to carry power from both conventional and renewable energy sources. The concepts presented in this paper can be applied in these scenarios.

## VI. CONCLUSION

Solar farms are idle during nights. A novel patent-pending control paradigm of PV solar farms is presented whereby they can be operated in nighttime as a STATCOM with full inverter capacity and during daytime with inverter capacity remaining after real power generation, for providing significant improvements in the power transfer limits of transmission systems [31,32]. This new control of PV solar system as STATCOM is termed PV-STATCOM. The effectiveness of the proposed controls is demonstrated on two study SMIB systems: System I having one 100 MW PV-STATCOM and System II having one 100 MW PV-STATCOM and another 100 MW PV-STATCOM or 100 MW wind farm controlled as STATCOM. Three different types of STATCOM controls are proposed for both the PV solar DG and inverter based wind DG. These are pure voltage control, pure damping control, and a combination of voltage control and damping control. The following conclusions are made:

- 1) In study system I, the power transfer can be increased by 168 MW during nighttime and by 142 MW in daytime even when the solar DG is generating a high amount of real power.
- 2) In Study System II, the transmission capacity in the night can be increased substantially by 229 MW if no DG is producing real power. During both nighttime and daytime, the power transfer can be increased substantially by 200 MW, even when the DGs are generating high real power.

This study thus makes a strong case for relaxing the present grid codes to allow selected inverter based renewable generators (solar and wind) to exercise damping control, thereby increasing much needed power transmission capability. Such novel controls on PV solar DGs (and inverter based wind DGs) will potentially reduce the need for investments in additional expensive devices such as series/shunt capacitors and FACTS.

The PV-STATCOM operation opens up a new opportunity for PV solar DGs to earn revenues in the nighttime and also daytime in addition to that from the sale of real power during the day. This will of course require appropriate agreements between the regulators, network utilities, solar farm developers and inverter manufacturers.

## VII. APPENDIX

Parameters of Solar and Wind Inverter Controllers:

PI1:  $K_p = 1$ ,  $T_i = 0.0015$ ; PI2:  $K_p = 1$ ,  $T_i = 0.1$ ; PI3:  $K_p = 2$ ,  $T_i = 0.2$ ;

PI4:  $K_p = 10$ ,  $T_i = 0.0015$ ;

Damping Controllers:  $T_v = 0.1$ ,  $G = 1.0$ ,  $T_1 = 1$ ,  $T_2 = 0.37$

## VIII. REFERENCES

- [1] R. M. Mathur and R. K. Varma, *Thyristor-Based FACTS Controllers for Electrical Transmission Systems*, New York: Wiley-IEEE Press, 2002.
- [2] Shah Arifur Rahman, Rajiv K. Varma and Wayne Litzemberger, "Bibliography of FACTS Applications for Grid Integration of Wind and PV Solar Power Systems: 1995-2010, IEEE Working Group Report", Paper 2011GM1483, Proc. IEEE PES GM, Detroit, USA, July 2011.
- [3] Ying Xiao, Y.H. Song, Chen-Ching Liu, Y.Z. Sun, "Available transfer capability enhancement using FACTS devices," *IEEE Transactions on Power Systems*, vol.18, no.1, pp. 305-312, Feb 2003.
- [4] [Online]. <http://www.crosstexas.com/>
- [5] Rajiv K. Varma, Vinod Khadkikar, and Ravi Seethapathy, "Nighttime application of PV solar farm as STATCOM to regulate grid voltage," *IEEE Trans. on Energy Conversion (Letters)*, vol. 24, no. 4, Dec. 2009.
- [6] Rajiv K. Varma and Vinod Khadkikar, "Utilization of Solar Farm Inverter as STATCOM" US Provisional Patent, filed 15 Sept. 2009.
- [7] R.K. Varma, S A Rahman, and R. Seethapathy, "Novel Control of Grid Connected Photovoltaic (PV) Solar Farm for Improving Transient Stability and Transmission Limits Both During Night and Day," in *Proc. 2010 World Energy Conference, Montreal, Canada*, pp. 1-6.
- [8] R.A. Walling and K. Clark, "Grid Support Functions implemented in Utility-Scale PV Systems," in *Proc. IEEE PES 2010, T&D Conf. and Exposition*, pp. 1-5.
- [9] F.L. Albuquerque, A.J. Moraes, G.C. Guimaraes, S.M.R. Sanhueza and A.R. Vaz, "Photovoltaic solar system connected to the electric power grid operating as active power generator and reactive power compensator," *Solar Energy*, vol. 84, no. 7, pp. 1310-1317, July 2010.
- [10] A. Beekmann, J. Marques, E. Quitmann, and S. Wachtel, "Wind energy converters with FACTS Capabilities for optimized integration of wind power into trans. and dist. systems", *CIGRE 2009, Calgary, Canada*.
- [11] Shah A Rahman, and R.K. Varma, "PSCAD/EMTDC Model of a 3-Phase Grid Connected Photovoltaic Solar System," in *Proc. 2011 43rd North American Power Symposium, Boston, U.S.A.*, pp. 1-5.
- [12] K.H. Hussein, I. Muta, T. Hoshino and M. Osakada "Maximum photovoltaic power tracking: an algorithm for rapidly changing atmospheric conditions", *IEE Proc.-Generation, Transmission and Distribution*, vol. 142, no. 1, pp. 59-64, January 1995.
- [13] Chatterjee, K., Fernandes, B.G., Dubey, G.K., "An instantaneous Reactive Volt-Ampere Compensator and Harmonic Suppressor System", *IEEE Trans. Power Electronics*, 1999, vol. 14-2, pp. 381-392.
- [14] M. H. Rashid, *Power Electronics Handbook*, Academic Press, 2001, pp. 355,363-364.
- [15] Seul-Ki Kim, Jin-Hong Jeon, Chang-Hee Cho, Eung-Sang Kim, Jong-Bo Ahn, "Modeling and simulation of a grid-connected PV generation system for electromagnetic transient analysis," *Solar Energy*, vol. 83, pp. 664-678, 2009.
- [16] A. Yazdani and R. Iravani, "Voltage-Sourced Converters in Power Systems-Modeling, Control and Applications," IEEE Press, John Wiley & Sons Inc. Publications, 2011
- [17] M. F. Schonardie and Denizar C. Martins, "Three-Phase Grid-Connected Photovoltaic System With Active And Reactive Power Control Using  $dq0$  Transformation," in *Proc. 2008 PESC*, pp. 1202-1207.
- [18] Z. Ye, R. Walling, L. Garces, R. Zhou, L. Li and T. Wang, "Study and Development of Anti-Islanding Control for Grid-Connected Inverters," GE Global Res. Center, New York, NREL/SR-560-36243, May 2004.
- [19] P. Kundur, *Power System Stability and Control*, McGraw Hill, New York, 1994
- [20] CIGRE Task Force 38.02.16, "Impact of Interactions among Power System Controls", *CIGRE Technical Brochure 166*, France, Aug. 2000.
- [21] Rajiv K. Varma, Ehsan Siavashi, Byomakesh Das, Vinay Sharma "Novel application of a PV Solar Plant as STATCOM during Night and Day in a Distribution Utility Network - Part 2", Panel Paper 2012 IEEE T&D Conference, May 2012, Orlando, USA
- [22] IEEE Standard for Interconnecting Distributed Resources With Electric Power Systems, Standard 1547-2003
- [23] [Online]. <http://www.pvresources.com/PVPowerPlants/Top50.aspx>
- [24] [Online] <http://energy.gov/articles/department-energy-offers-conditional-loan-guarantee-commitments-support-nearly-45-billion>
- [25] [Online]. <http://www.firstsolar.com/Projects/Projects-Under-Development/Desert-Sunlight-Solar-Farm/Overview>
- [26] [Online]. [http://www.blm.gov/pgdata/etc/medialib/blm/ca/pdf/palmsprings/desert\\_sunlight.Par.38926.File.dat/Chapter-2.0\\_Project-Description-Draft-EIS-DesertSunlightSolarProject.pdf](http://www.blm.gov/pgdata/etc/medialib/blm/ca/pdf/palmsprings/desert_sunlight.Par.38926.File.dat/Chapter-2.0_Project-Description-Draft-EIS-DesertSunlightSolarProject.pdf)
- [27] [Online]. [http://www.samsungrenewableenergy.ca/sites/default/files/pdf/GREP\\_ConstructionPlanReport.pdf](http://www.samsungrenewableenergy.ca/sites/default/files/pdf/GREP_ConstructionPlanReport.pdf)
- [28] [Online]. [http://www.globaltransmission.info/archive\\_main.php?id=18&region=1](http://www.globaltransmission.info/archive_main.php?id=18&region=1)
- [29] [Online]. <http://www.swipos.com/about.htm>
- [30] [Online]. [http://tdworld.com/overhead\\_transmission/bpa-high-voltage-power-line-wa-20110501/](http://tdworld.com/overhead_transmission/bpa-high-voltage-power-line-wa-20110501/)
- [31] R. K. Varma and Shah Arifur Rahman, "Novel Control of Inverter based DGs as FACTS (DGFACTS) for Enhancing Grid Power Transmission Limits, US Provisional Patent No. 61/309,612 filed 2<sup>nd</sup> March 2010.
- [32] Rajiv K. Varma, Vinod Khadkikar and Shah Arifur Rahman, "Utilization of Distributed Generator Inverters as STATCOM" PCT Patent application PCT/CA2010/001419 filed on 15 September, 2010.

## BIOGRAPHY



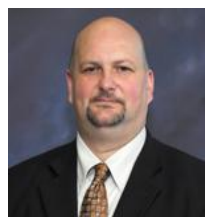
**Rajiv K. Varma** (SMIEEE 2009) obtained B.Tech. and Ph.D. degrees in Electrical Engineering from Indian Institute of Technology (IIT), Kanpur, India, in 1980 and 1988, respectively. He is currently Associate Professor and Hydro One Chair in Power Systems Engineering at the University of Western Ontario (UWO), Canada. Prior to this position, he was a faculty member in the Electrical Engineering Department at IIT Kanpur, India, from 1989-

2001. He has co-authored an IEEE Press/Wiley book on Thyristor Based FACTS Controllers. He is active on a number of IEEE working groups. He has co-delivered several Tutorials on SVC sponsored by IEEE Substations Committee. His research interests include FACTS, power systems stability, and grid integration of wind and photovoltaic solar power systems. He was a member of the IEEE Working Group on "HVDC and FACTS Bibliography and Records" during 1994-1998. He is now the Chair of IEEE Working Group 15.05.17 on "HVDC and FACTS Bibliography," since 2004.



**Shah Arifur Rahman** (MIEEE 2013) received his Ph.D. degree from the University of Western Ontario, London, ON, Canada. He is currently working as a Post-Doctoral Fellow with the University and performing research activities at Bluewater Power, Sarnia. His research interests include grid integration of inverter based Distributed Generation (DG) sources such as photovoltaic (PV) solar plants, wind farms, energy storage etc., impact analysis of harmonics and

overvoltages on power systems, implementation of FACTS capability in inverter based DGs and their coordination. He is a member of the IEEE Working Group on "HVDC and FACTS Bibliography and Records" since 2010 and acting as Secretary since 2012.



**Tim Vanderheide** holds the position of Chief Operating Officer for both Bluewater Power Renewable Energy Inc. and Electek Power Services Inc. Tim is also Vice President of Strategic Planning for Bluewater Power Distribution Corporation. Tim is responsible for the development and implementation of renewable power generation projects for Bluewater Power Renewable Energy Inc. as well as the development

of new product and service strategies designed to continuously improve shareholder value for Bluewater Power Distribution. In his role as Chief Operating Officer for Electek Power Services Inc., Tim is responsible for overall operations and company growth. Prior to his current positions, Tim was Vice-President of Client Services for Bluewater Power Distribution Corporation. In this role, Tim was responsible for market services, energy services, metering, billing and information technologies.